Resonance phenomena in asymmetric superconducting quantum interference devices

T. P. Polak and E. Sarnelli

Consiglio Nazionale delle Ricerche-Istituto Nazionale per la Fisica della Materia, Complesso Universitario Monte S. Angelo, 80126 Naples, Italy and Istituto di Cibernetica "E. Caianiello" del CNR, Via Campi Flegrei 34, I-80078 Pozzuoli, Italy

(Received 2 January 2007; revised manuscript received 21 April 2007; published 30 July 2007)

The theory of self-induced resonances in asymmetric two-junction interferometer device is presented. In real devices, it is impossible to have an ideal interferometer free of imperfections. Thus, we extended previous theoretical approaches, introducing a model that contains several asymmetries: Josephson current ϵ, capacitances χ, and dissipation ρ presented in an equivalent circuit. Moreover, nonconventional symmetry of the order parameter in high temperature superconducting quantum interference devices forced us to include phase asymmetries. Therefore, the model has been extended to the case of π-shift interferometers, where a phase shift is present in one of the junctions.

DOI: 10.1103/PhysRevB.76.014531 PACS number(s): 74.72.−h, 74.50.+r

I. INTRODUCTION

Superconducting quantum interference devices (SQUIDs) are the most employed superconductive electronic circuits in practical applications.[1–9] With the discovery of high-temperature superconductors (HTSs), high-temperature SQUIDs have also been developed.[10–14] This class of devices, although less sensitive than the most competitive low-temperature SQUIDs, has been used in several applications, where portability and/or positioning as much as high working temperatures are needed. Moreover, the demonstration of an unconventional symmetry of the order parameter in YBaCuO (Refs. 15–17) opened new horizons for using the so-called π-SQUIDs in superconductive electronics. Indeed, π-SQUIDs[18] can be used to self-frustrate quantum bit circuits or to feed rapid single flux quantum devices.[19,20] As a consequence, a full knowledge of the properties of HTS SQUIDs is of great importance. In particular, the aspects limiting their utilization in applications have to be explored. We can consider two effects limiting performance of HTS zero- or π-SQUIDs (zero indicates the conventional SQUID where no phase shift has been established along the superconducting loop): asymmetries in the junction properties and anomalous electrical behavior induced by an arbitrary phase shift in one of the two junctions forming the interferometer. Asymmetries in conventional low-temperature devices have been first examined by Tesche and Clarke.[21] In their paper, a complete study of the performance in terms of noise characteristics has been carried out. The interest on asymmetric SQUIDs grew up again after the discovery of HTS. Indeed, the parameter spread in HTS SQUIDs is often so large that significant asymmetries arise. Hence, it is particularly hard to fabricate two identical HTS Josephson junctions, even though they are very close to each other on the chip. Performance of asymmetric SQUIDs has been analyzed by Testa *et al.*.[22,23] From their papers, it is evident that higher magnetic sensitivities are achieved when asymmetric SQUIDs are used. The asymmetry combined with a damping resistance leads to a flux to voltage transfer coefficient several times larger than the one typical for symmetric devices, together with a lower magnetic flux noise. The large ratio of the flux to voltage transfer coefficient allows a direct coupling to an external preamplifier without the need of an impedance matching flux transformer or additional positive feedback circuitry. This simplifies the readout electronics, as required in multichannel systems for low-noise measurements. However, the final performance of a dc-SQUID is influenced by the presence of undesired anomalies occurring on the current-voltage (*IV*) characteristics, namely, Fiske or resonant steps.[24] Such structures originate from the nonlinear interaction between the resonant cavity, represented by the superconducting loop, and an rf current component, the ac Josephson current in the junctions. This system may be treated with the equivalent electrical resonant circuit, as shown in Fig. 1.

A deep investigation of the properties of resonances in asymmetric SQUIDs, also including different phase shift in the SQUID loop, is mandatory and can be very useful for people involved in SQUID design. Self-resonances occurring in superconducting interferometers are considered to be phenomena reducing performance of high-sensitivity SQUIDs. Indeed, Zappe and Landman[25] first investigated experimentally resonances in low-Q Josephson interferometers. The analysis was taken again by Tuckerman and Magerlein,[26] who presented a theoretical and experimental investigation of resonances in symmetric devices. Successively, Faris and Valsamakis[27] showed characteristic of resonances in asymmetric two-junction interferometers, introducing an important distinction between current- and voltage-controlled cases. Based on their analysis, Camerlingo *et al.*[28] reported an experimental work showing the effect of the loop capacitance on resonant voltages in asymmetric interferometers. Recently, the nature of resonances in SQUIDs in which a significant flux is coupled to the Josephson junctions, called spatially distributed junctions dc-SQUID, has been analyzed by Chesca.[29] He showed that useful information about the order parameter symmetry can be provided by studying directly the magnetic field dependences of both the dc Josephson critical current and self-induced resonant modes of dc-SQUIDs made of nonconventional superconductors. Further analysis of voltage states in current-voltage characteristics of symmetric dc π-SQUIDs, in which the junctions are equal and not-distributed circuital elements, has been done by Chesca and Kleiner.[30] Moreover, *d*-wave induced zero-field

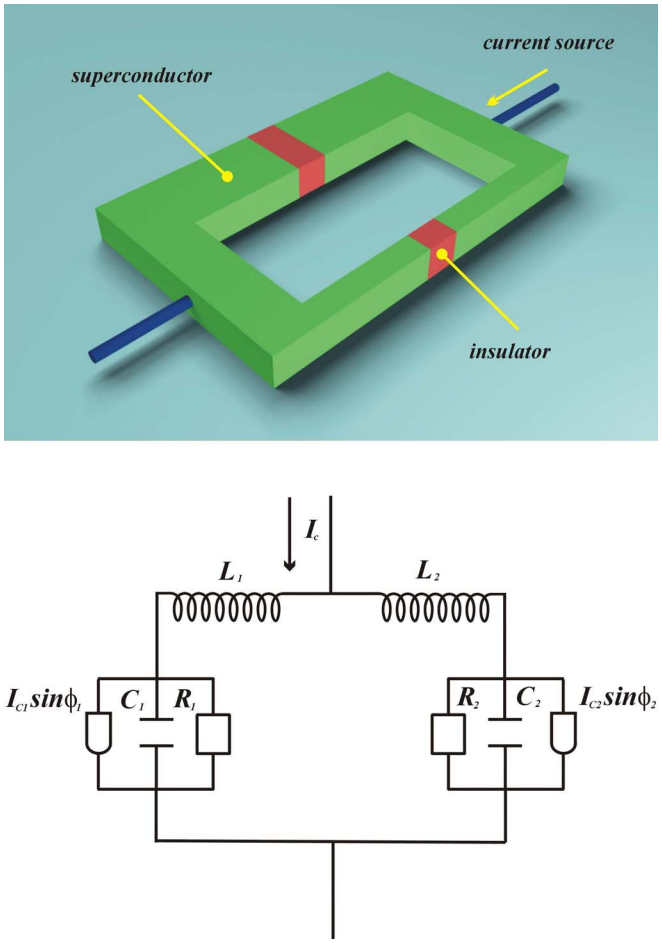

FIG. 1. (Color online) Theoretical model of an asymmetric superconducting quantum interference device and the equivalent circuit contains two Josephson junctions with the critical current I_{C_i} and parallel capacitance C_i. Each single junction contains parallel linear resistance R_i and the interferometer is fed by an external source I_c. The self-inductances of the junctions are equal to L_i and ϕ_i is the phase difference across the ith junction.

resonances in dc π-SQUIDs have also been observed.[31]

In our work, we present a full investigation of resonances in asymmetric SQUIDs, also in the presence of asymmetries in the junction phases. The outline of the paper is the following: In Sec. II, we outline the model Hamiltonian, and we derive equations for asymmetric dc-SQUIDs. In Sec III, we present the method and assumptions which have been made. In Sec. IV, we present our results considering special cases and their relevance to the other theoretical works. Finally, in Sec. V we discuss the relevance of the obtained results to the experimental situations.

II. MODEL

We start with defining an asymmetric superconducting quantum interference device (ASQUID) which consists of two Josephson junctions (see Fig. 1). Each of them has a critical current I_{C_i} and a parallel capacitance C_i. We assume also that a single junction contains a parallel linear resistance R_i and interferometer is fed by an external source I_c, but the details of the equivalent circuit will be specified later. The self-inductances of the junctions in ASQUID are equal to L_1 and L_2. We do not consider mutual inductances between the junctions. The Hamiltonian of the ASQUID contains three parts:[24,32]

$$\mathcal{H} = \mathcal{H}_C + \mathcal{H}_J + \mathcal{H}_M. \tag{1}$$

The first term on the right side of Eq. (1) defines the electrostatic energy,

$$\mathcal{H}_C = \frac{1}{2}C_1V_1^2 + \frac{1}{2}C_2V_2^2, \tag{2}$$

where V_i is the voltage across the ith junction. The last equation can be transformed to the phase representation using the Josephson relation $\dot{\phi}=2\pi/\Phi_0 V$:

$$\mathcal{H}_C = \frac{1}{2}\left(\frac{\Phi_0}{2\pi}\right)^2(C_1\dot{\phi}_1^2 + C_2\dot{\phi}_2^2), \tag{3}$$

where ϕ_i is a phase difference across the ith junction. The second term is the Josephson energy,

$$\mathcal{H}_J = E_{J,1}(1-\cos\phi_1) + E_{J,2}(1-\cos\phi_2), \tag{4}$$

where $E_{J,i}=\Phi_0/2\pi I_{C,i}$. To complete the set of equations for the interferometer, one should take into account that loop current I_L can contribute to the flux. The gauge invariant superconducting phase differences between the edges of any loop and magnetic flux are directly related by the fluxoid quantization relation:

$$\phi_2 - \phi_1 = 2\pi n + \phi_{ext} - \frac{2\pi}{\Phi_0}L_+I_L, \tag{5}$$

where n is an integer and

$$L_+ = L_1 + L_2, \tag{6}$$

$$I_L = \frac{L_1I_1 - L_2I_2}{L_+}. \tag{7}$$

Finally, for $n=0$ magnetic energy takes the form

$$\mathcal{H}_M = \frac{1}{2}L_+I_L^2 = \frac{1}{2}\left(\frac{\Phi_0}{2\pi}\right)^2\frac{(\phi_2-\phi_1-\phi_{ext})^2}{L_+}. \tag{8}$$

At this stage, we do not provide an information about dissipative environment and external forces which will be discussed later. Applying the Euler-Lagrange equation

$$dt(\partial_{\dot{\phi}_n}\mathcal{L}) - \partial_{\phi_n}\mathcal{L} = 0 \tag{9}$$

to the Lagrangian

$$\mathcal{L} = \frac{1}{2}\left(\frac{\Phi_0}{2\pi}\right)^2(C_1\dot{\phi}_1^2 + C_2\dot{\phi}_2^2) - \frac{1}{2}\left(\frac{\Phi_0}{2\pi}\right)^2\frac{(\phi_2-\phi_1-\phi_{ext})^2}{L_+} - E_{J,1}(1-\cos\phi_1) - E_{J,2}(1-\cos\phi_2), \tag{10}$$

we find equations of motion

$$\left(\frac{\Phi_0}{2\pi}\right)^2 C_1\ddot{\phi}_1 + E_{J1}\sin\phi_1 = \left(\frac{\Phi_0}{2\pi}\right)^2\frac{(\phi_2-\phi_1)}{L_+}, \tag{11}$$

$$\left(\frac{\Phi_0}{2\pi}\right)^2 C_2\ddot{\phi}_2 + E_{J,2}\sin\phi_2 = \left(\frac{\Phi_0}{2\pi}\right)^2 \frac{(\phi_1-\phi_2)}{L_+}. \quad (12)$$

Similar to Tesche and Clarke,[21] we introduce the following parameters:

$$C_1 = (1+\chi)C, \quad C_2 = (1-\chi)C, \quad (13)$$

$$E_{J,1} = (1+\epsilon)E_J, \quad E_{J,2} = (1-\epsilon)E_J, \quad (14)$$

$$L_1 = (1+\lambda)\frac{L}{2}, \quad L_2 = (1-\lambda)\frac{L}{2}, \quad (15)$$

where dimensionless anisotropy quantities χ, ϵ, and λ describe the relative deviations of the model parameters from the corresponding average values C, E_J, and L. We can vary the values of the anisotropy parameters within the range [0, 1), where zero leads to the isotropic model and value 1 completely rules out the presence of one junction from the interferometer. Since $L_+=L$, we conclude that a difference between inductances does not influence the dynamics of the model. After renormalization to dimensionless quantities

$$\omega_c^2 = \left(\frac{2\pi}{\Phi_0}\right)^2 \frac{E_J}{C} = \frac{1}{LC}, \quad (16)$$

$$\beta = \frac{2\pi}{\Phi_0} I_C L, \quad (17)$$

we finally obtain two coupled nonlinear second-order differential equations describing an ASQUID:

$$(1-\chi)\ddot{\phi}_1 + (1-\epsilon)\sin(\phi_1+\vartheta_1) = \frac{(\phi_2-\phi_1)}{\beta}, \quad (18)$$

$$(1-\chi)\ddot{\phi}_2 + (1+\epsilon)\sin(\phi_2+\vartheta_2) = \frac{(\phi_1-\phi_2)}{\beta}. \quad (19)$$

Until now, we have not considered dissipation effects and specific geometry of the circuit. First, we have to decide what modes of operation to use: current controlled or voltage controlled (VC). This is a crucial point simply because a choice we make is going to affect our system. For the VC case where SQUID is excited by a voltage source V_s, we have to add terms proportional to $V_s t$ to the equations. The difference caused by various excitation sources affects frequencies of the oscillating modes of the system. In this paper, we assume that SQUID is current excited by a constant current source (see Fig. 1). This foundation leads to an additional term γ_i in both equations. The origin of the last parameter is clear when we consider the equivalent loop of a real interferometer[26] where the center of the inductance is fed by a gate current source I_g. Using notation from the paper of Tuckerman and Magerlein and the above information, we can derive the exact form of γ_i:

$$\gamma_1 = \frac{I_g + 2I_c}{2I_C}, \quad \gamma_2 = \frac{I_g - 2I_c}{2I_C}, \quad (20)$$

where I_c is a circulating current.

Considering dissipation due to a quasiparticle current, we add parallel resistances R_i. These dissipative currents flowing through the junctions of the interferometer can vary from each other and, as a consequence, we have to introduce their asymmetry assuming

$$(1+\rho)\alpha = \left(\frac{\Phi_0}{2\pi}\right)^2 \frac{1}{R_1}, \quad (1-\rho)\alpha = \left(\frac{\Phi_0}{2\pi}\right)^2 \frac{1}{R_2}. \quad (21)$$

Different phase shift can be added to each junction separately putting $\phi_i+\vartheta_i$ in Eqs. (18) and (19). We see that values $\vartheta_0=0$ and $\vartheta_1=\pi$ lead to the opposite sign of the current which means its opposite direction. Finally, we write the equations for ASQUID with phase shift in the form

$$(1+\chi)\ddot{\phi}_1 + (1+\rho)\alpha\dot{\phi}_1 + (1+\epsilon)\sin(\phi_1+\vartheta_1) = \gamma_1 + \frac{(\phi_2-\phi_1)}{\beta}, \quad (22)$$

$$(1-\chi)\ddot{\phi}_2 + (1-\rho)\alpha\dot{\phi}_2 + (1-\epsilon)\sin(\phi_2+\vartheta_2) = \gamma_2 + \frac{(\phi_1-\phi_2)}{\beta}. \quad (23)$$

In order to obtain similar node equations, one can also use Kirchoff's current law to the specific circuit. We have to mention that the noise effects are not present in our analysis. Choice of parameters $\chi=\epsilon=\rho=\vartheta=0$ stands for the fully symmetric case.

III. METHOD

We shall analyze two coupled differential equations [Eqs. (22) and (23)] for the case $\beta \leqslant 1$ that coupling between the two junctions of the interferometer is strong, and hence, the last terms of the right hand of Eqs. (22) and (23) play an important role since they contain expressions proportional to $\pm\beta^{-1}(\phi_2-\phi_1)$. Let us introduce new variables

$$\phi_- = \frac{\phi_1-\phi_2}{2}, \quad \phi_+ = \frac{\phi_1+\phi_2}{2}, \quad (24)$$

$$\gamma_- = \frac{\gamma_1-\gamma_2}{2}, \quad \gamma_+ = \frac{\gamma_1+\gamma_2}{2}, \quad (25)$$

$$\vartheta_- = \frac{\vartheta_1-\vartheta_2}{2}, \quad \vartheta_+ = \frac{\vartheta_1+\vartheta_2}{2}, \quad (26)$$

where ϕ_- represents the flux number (this parameter distinguishes interferometer from a point junction), and ϕ_+ is the average phase difference of the junctions. For the equivalent circuit of a real interferometer, γ_- can be recognized as a control current I_c and γ_+ as a bias current I_g. Parameters $\vartheta_\pm$ are relative changes of the phase shifts present in each junction. In terms of the above, we write Eqs. (22) and (23) in the form

$$\ddot{\phi}_+ + \alpha\dot{\phi}_+ + \sin(\phi_+ + \vartheta_+)\cos(\phi_- + \vartheta_-) - \gamma_+ + \chi\ddot{\phi}_- + \alpha\rho\dot{\phi}_- + \epsilon\sin(\phi_- + \vartheta_-)\cos(\phi_+ + \vartheta_+) = 0, \quad (27)$$

$$\ddot{\phi}_- + \alpha\dot{\phi}_- + \sin(\phi_- + \vartheta_-)\cos(\phi_+ + \vartheta_+) - \gamma_- + \frac{2}{\beta}\phi_- + \chi\ddot{\phi}_+ + \alpha\rho\dot{\phi}_+ + \epsilon\sin(\phi_+ + \vartheta_+)\cos(\phi_- + \vartheta_-) = 0. \quad (28)$$

In the following, we have to assume a form of the solution. The voltage variations appearing in ASQUID come from the interaction between the junction current and circuit's elements. We assume voltage sinusoidal variations with dc component V, ac amplitude v, frequency ω, and phase φ:

$$V(t) = V + v\cos(\omega t + \varphi), \quad (29)$$

where other harmonics are filtered out. Using the Josephson relations and integrating out, we get for the ith junction

$$\phi_i(t) = \phi_{0,i} + \omega t \pm \delta\sin(\omega t + \varphi), \quad (30)$$

where $\delta = \frac{v}{V}$. The flux number ϕ_- and the average phase difference ϕ_+ can be written as

$$\phi_- = \phi_c - \delta\sin\omega t, \quad (31)$$

$$\phi_+ = n\omega t - \theta, \quad (32)$$

where ϕ_c is the average value of the internal phase ϕ_-. In order to account the difference between odd and even behavior of the ASQUID interferometer, we define

$$\phi_- = \phi_c - \delta\sin\omega t - k\frac{\pi}{2}, \quad (33)$$

$$\phi_+ = n\omega t - \theta - k\frac{\pi}{2}, \quad (34)$$

where k is equal to 0 (1) for even (odd) number of resonances.

IV. RESULTS

Substituting expressions (33) and (34) into Eqs. (27) and (28) and extracting by calculating average over time the dc, $\sin\omega t$, and $\cos\omega t$ Fourier components, we get

$$\alpha n\omega = \gamma_+ - J_n(\delta)\cos(\theta - \vartheta_+)\sin(\phi_c + \vartheta_-) + \epsilon J_n(\delta)\sin(\theta - \vartheta_+)\cos(\phi_c + \vartheta_-), \quad (35)$$

$$\gamma_- = \frac{2}{\beta}\phi_c - J_n(\delta)\sin(\theta - \vartheta_+)\cos(\phi_c + \vartheta_-) + \alpha\rho n\omega + \epsilon J_n(\delta)\cos(\theta - \vartheta_+)\sin(\phi_c + \vartheta_-), \quad (36)$$

$$-\chi\delta\omega^2 = J_n^-(\delta)\cos(\theta - \vartheta_+)\cos(\phi_c + \vartheta_-) + \epsilon J_n^-(\delta)\sin(\theta - \vartheta_+)\sin(\phi_c + \vartheta_-), \quad (37)$$

$$\alpha\rho\delta\omega = -J_n^+(\delta)\sin(\theta - \vartheta_+)\cos(\phi_c + \vartheta_-) + \epsilon J_n^+(\delta)\cos(\theta - \vartheta_+)\sin(\phi_c + \vartheta_-), \quad (38)$$

$$\delta\left(\frac{2}{\beta} - \omega^2\right) = J_n^-(\delta)\sin(\theta - \vartheta_+)\sin(\phi_c + \vartheta_-) + \epsilon J_n^-(\delta)\cos(\theta - \vartheta_+)\cos(\phi_c + \vartheta_-), \quad (39)$$

$$\alpha\delta\omega = J_n^+(\delta)\cos(\theta - \vartheta_+)\sin(\phi_c + \vartheta_-) - \epsilon J_n^+(\delta)\sin(\theta - \vartheta_+)\cos(\phi_c + \vartheta_-), \quad (40)$$

where

$$J_n^\pm(\delta) = J_{n-1}(\delta) \pm J_{n+1}(\delta) \quad (41)$$

and $J_n(\delta)$ is the Bessel function of the first kind.[33] Using Eqs. (35) and (40) and the Bessel function identity, we obtain

$$\alpha n\omega = \gamma_+ - \frac{J_n(\delta)}{J_n^+(\delta)}\alpha\delta\omega = \gamma_+ - \frac{\alpha\delta^2\omega}{2n}. \quad (42)$$

We define normalized excess current due to the resonance

$$I_{exc} = \frac{\alpha\delta^2\omega}{2n}. \quad (43)$$

The above equations can be rewritten using the dimensionless damping parameter $\Gamma \equiv (\alpha\omega_r)^{-1}$, where ω_r is the resonant frequency. Γ was introduced by Werthamer and Shapiro[34] and described the strength of the coupling of the current to the resonance in the case of the junction coupled to cavity. Several authors used it as a damping parameter.[25,26] We can combine Eqs. (36) and (38),

$$\gamma_- = \frac{2}{\beta}\phi_c + \alpha\rho n\omega + \frac{\alpha\rho\delta^2\omega}{2n}, \quad (44)$$

and using relation for excess current, we get

$$\gamma_- = \frac{2}{\beta}\phi_c + \rho\gamma_+. \quad (45)$$

We see that formula (43) for excess current is universal in such sense that it holds even for asymmetric SQUID. This expression is also true in the presence of any changes of the phase shift in one of the junctions of the interferometer. We can add squares of expressions (37)–(40):

$$\left[\frac{\delta(1-\tilde{\omega}^2)}{J_n^-(\delta)}\right]^2 + \left[\frac{\alpha\delta\tilde{\omega}}{J_n^+(\delta)}\right]^2 + \left[\frac{\chi\delta\tilde{\omega}^2}{J_n^-(\delta)}\right]^2 + \left[\frac{\alpha\rho\delta\tilde{\omega}}{J_n^+(\delta)}\right]^2 = 1 + \epsilon^2, \quad (46)$$

where $\tilde{\omega} = \omega/\omega_r = V/V_r$ is the normalized voltage. From above and Eq. (43), we can derive normalized excess current dependence on voltage for given anisotropic parameters. However, analysis is complex and it is better to simplify our model considering special cases which could give us more insight into the structure of resonances in ASQUID.

A. Special cases

For a general choice of parameters, Eqs. (35)–(40) are coupled and must be solved numerically. However, considerations of special cases can provide more insights into general solution of the problem.

1. Asymmetry of the Josephson current ($\epsilon \neq 0$)

In this case, we assume that only Josephson current asymmetry is present. Then, Eq. (46) can be reduced to the form

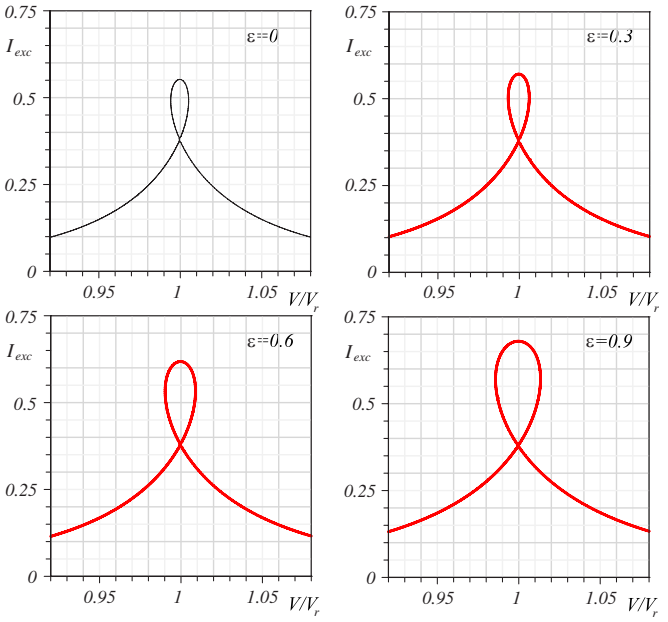

FIG. 2. (Color online) Current-voltage characteristics with Josephson current anisotropy ϵ, for the first resonance, $\Gamma=20$, and $\beta=0.1$. The black color of the curves used in this and the next plots indicates the symmetric SQUID $\chi=\epsilon=\rho=0$.

$$\left[\frac{\delta(1-\tilde{\omega}^2)}{J_n^-(\delta)}\right]^2+\left[\frac{\alpha\delta\tilde{\omega}}{J_n^+(\delta)}\right]^2=1+\epsilon^2. \tag{47}$$

From the above expression coupled with Eq. (43), we can derive the normalized current dependence on normalized voltage plots with ϵ asymmetry (see Fig. 2). Also, the normalized resonant current versus damping parameter for several resonances can be obtained (see Fig. 3).

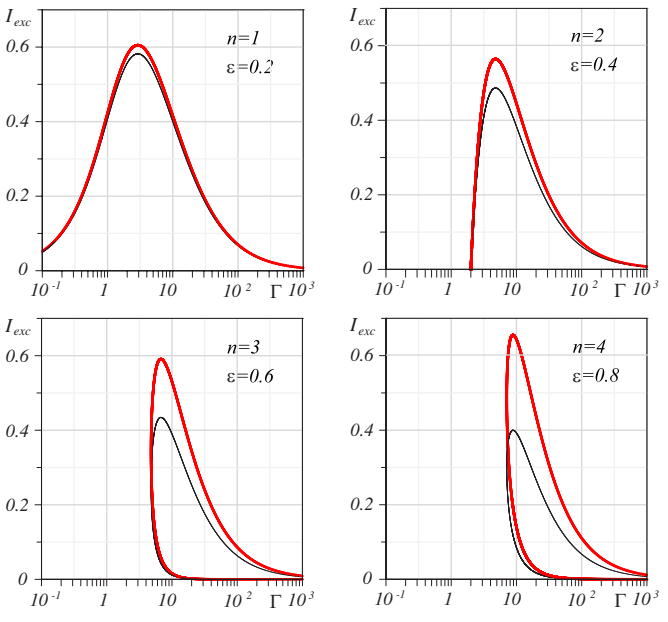

FIG. 3. (Color online) The normalized resonant current I_{exc} versus damping parameter Γ for different values of the Josephson current anisotropy parameters ϵ (red curves), for the nth resonance.

2. Asymmetry of the capacitances ($\chi\neq0$) and resistances ($\rho\neq0$) with phase shift ($\vartheta_\pm\neq0$)

Let us consider the case when $\epsilon=0$, which means that asymmetry of the Josephson current is not present. In this case, Eqs. (35)–(40) are reduced to

$$\alpha n\omega=\gamma_+-J_n(\delta)\cos(\theta-\vartheta_+)\sin(\phi_c+\vartheta_-), \tag{48}$$

$$\gamma_-=\frac{2}{\beta}\phi_c-J_n(\delta)\sin(\theta-\vartheta_+)\cos(\phi_c+\vartheta_-)+\alpha\rho n\omega, \tag{49}$$

$$-\chi\delta\omega^2=J_n^-(\delta)\cos(\theta-\vartheta_+)\cos(\phi_c+\vartheta_-), \tag{50}$$

$$\alpha\rho\delta\omega=-J_n^+(\delta)\sin(\theta-\vartheta_+)\cos(\phi_c+\vartheta_-), \tag{51}$$

$$\delta\left(\frac{2}{\beta}-\omega^2\right)=J_n^-(\delta)\sin(\theta-\vartheta_+)\sin(\phi_c+\vartheta_-), \tag{52}$$

$$\alpha\delta\omega=J_n^+(\delta)\cos(\theta-\vartheta_+)\sin(\phi_c+\vartheta_-). \tag{53}$$

First, we will analyze the low-Γ case in order to compare our results with the original calculations presented in literature.[25,35]

Low-Γ devices with symmetric values of the Josephson current ($\epsilon=0$). At the resonance frequency $\omega=n\omega_r$ Eq. (52) is satisfied when $\theta=\vartheta_+$. This condition rules out equations with terms proportional to $\sin(\theta-\vartheta_+)$, and therefore there is no trace of the asymmetries of the Josephson current ϵ and dissipation ρ. For low-Γ devices, $J_n^\pm(\delta)=0$ for $n>1$, and hence only the first resonance exists. We can derive the following equations:

$$-\frac{\delta}{\Upsilon}=\cos(\phi_c+\vartheta_-), \tag{54}$$

$$\frac{\delta}{\Gamma}=\sin(\phi_c+\vartheta_-), \tag{55}$$

where $\Upsilon\equiv(\chi\omega^2)^{-1}$ is a dimensionless parameter. Rearranging the last equation and putting into expression for excess current, we get

$$I_{exc}=\Gamma\sin^2(\phi_c+\vartheta_-), \tag{56}$$

which is a general result for different SQUIDs. We can calculate other relations,

$$I_{exc}=\frac{\Upsilon^2}{\Gamma}\cos^2(\phi_c+\vartheta_-), \tag{57}$$

$$\frac{\Upsilon}{\Gamma}=-\tan(\phi_c+\vartheta_-), \tag{58}$$

which are plotted in Fig. 4. We see that the results obtained previously by other authors[25,35] are presented in the framework of our rather general calculations and can be derived as special cases.

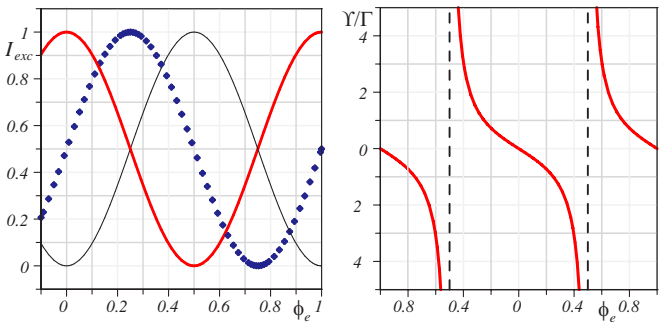

FIG. 4. (Color online) Dependence of the normalized resonant current I_{exc} with relative phase shift $\vartheta_-=0.5$ (red), 0.25 (dot), and 0 (black) and the ratio Υ/Γ with no phase shift $\vartheta_-=0$ versus magnetic field ϕ_c.

Analysis for not small Γ. When Γ is not small, we cannot simplify equations using condition under which Bessel functions can be approximated by zero except the case of the first resonance. Putting $\epsilon=0$ in Eq. (46), we obtain

$$\left[\frac{\delta(1-\tilde{\omega}^2)}{J_n^-(\delta)}\right]^2+\left[\frac{\alpha\delta\tilde{\omega}}{J_n^+(\delta)}\right]^2+\left[\frac{\chi\delta\tilde{\omega}^2}{J_n^-(\delta)}\right]^2+\left[\frac{\alpha\rho\delta\tilde{\omega}}{J_n^+(\delta)}\right]^2=1. \tag{59}$$

From the above equation and expression (43) for the excess current, we can derive the normalized current voltage characteristics for ASQUID. The second and the fourth terms of the above equation can be combined. We see that the influence of the anisotropy of the dissipative current,

$$\left[\frac{\alpha\delta\tilde{\omega}}{J_n^+(\delta)}\right]^2\rightarrow[1+\rho]\left[\frac{\alpha\delta\tilde{\omega}}{J_n^+(\delta)}\right]^2, \tag{60}$$

manifests by the decrease of the maximum value of the resonant current, for a given nth resonance mode, when we increase the anisotropy parameter ρ (see Figs. 5 and 6). We observe a shift of the maximum value of I_{exc} toward higher values of the damping parameter Γ. Analysis of the influence of the anisotropy of the capacitances can be done in the same manner. We can again merge the first and third terms of Eq. (59). Contrary to the previous simple case, the present one is more complex merely because we have taken into account element proportional to $\tilde{\omega}^4$, which produces minor changes (see Figs. 7 and 8). Now, even small deviations of the anisotropy parameter χ from equilibrium have a major impact on equations and, in consequence, on the behavior of the ASQUID. For small values of χ, at fixed value of the damping parameter Γ there are two possible solutions even for the first resonance. In symmetric SQUIDs, this situation was present for higher resonances $n\geqslant 3$. Explanation of the latter comes from the fact that the resonant circuit oscillates at a frequency of ω_r, while Josephson current in the junctions oscillates at $n\omega_r$. In ASQUID, we have three natural frequencies[27] $\omega_{1,2}=(L_+C_{1,2})^{-1/2}$ and related $\omega_3^2=\omega_1^2+\omega_2^2$ which can be excited by the ac Josephson effect and converted through nonlinear interactions between junction and resonant circuit into dc current steps. Therefore, introducing capacitance anisotropy, we are able to create higher mode multivalued behavior of the excess current even for the first resonance (Fig. 9).

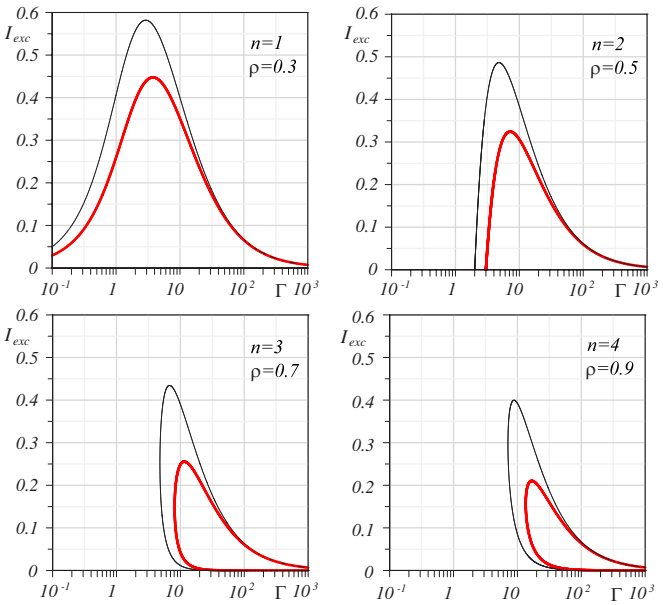

FIG. 5. (Color online) The normalized resonant current I_{exc} versus damping parameter Γ for different values of the dissipation anisotropy parameters ρ (red curves), for the nth resonance.

3. Symmetric case ($\chi=\epsilon=\rho=0$) with phase shift ($\vartheta_\pm\neq 0$)

This case corresponds with a situation where different phase shift is present in the junctions of the interferometer and analysis is similar to the one carried by Chesca.[29] The equations take the form

$$\alpha n\omega=\gamma_+-J_n(\delta)\cos(\theta-\vartheta_+)\sin(\phi_c+\vartheta_-), \tag{61}$$

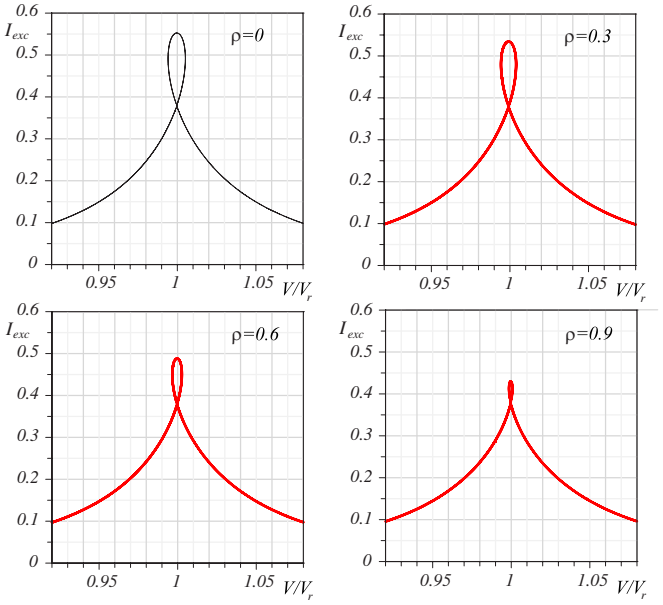

FIG. 6. (Color online) Current-voltage (I_{exc}-V/V_r) characteristics with dissipation anisotropy ρ, for the first resonance ($n=1$), $\Gamma=20$, and $\beta=0.1$.

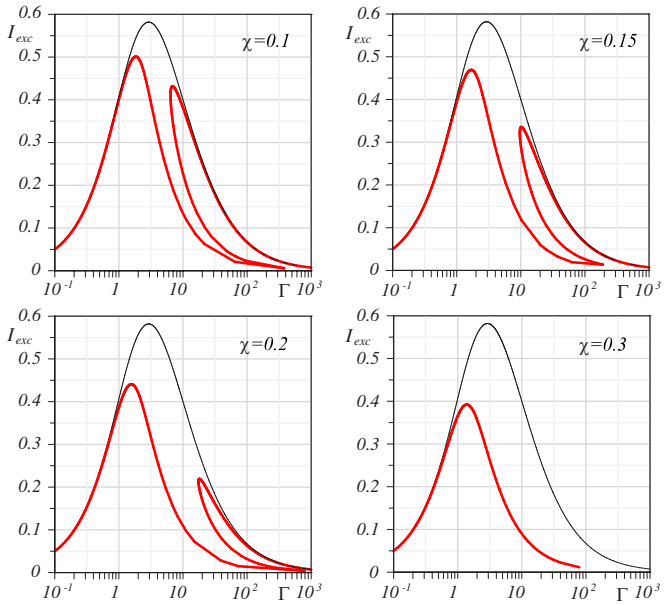

FIG. 7. (Color online) The normalized resonant current I_{exc} versus damping parameter Γ, for different capacitance anisotropy parameters χ and for the first resonance ($n=1$).

$$\gamma_- = \frac{2}{\beta}\phi_c - J_n(\delta)\sin(\theta - \vartheta_+)\cos(\phi_c + \vartheta_-), \tag{62}$$

$$\delta\left(\frac{2}{\beta} - \omega^2\right) = J_n^-(\delta)\sin(\theta - \vartheta_+)\sin(\phi_c + \vartheta_-), \tag{63}$$

$$\alpha\delta\omega = J_n^+(\delta)\cos(\theta - \vartheta_+)\sin(\phi_c + \vartheta_-). \tag{64}$$

We do not expect any changes in excess current-voltage characteristics. Rather, as it was pointed out by Chesca, the

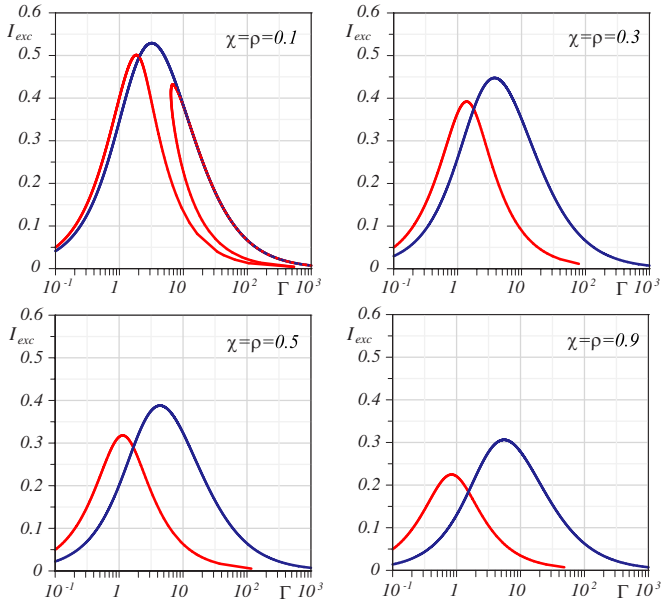

FIG. 8. (Color online) The normalized resonant current I_{exc} versus damping parameter Γ, for different values of the capacitance and dissipation anisotropy parameters $\chi(\text{red})=\rho(\text{blue})$ and for the first resonance ($n=1$).

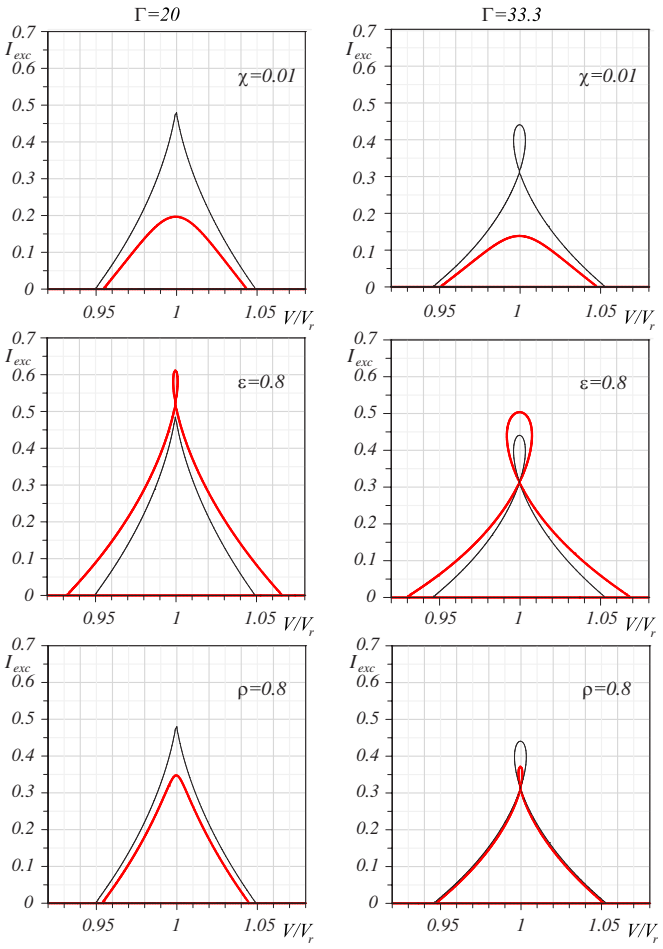

FIG. 9. (Color online) The normalized resonant current I_{exc} versus normalized voltage V/V_r, with different values of the anisotropy parameters, capacitance χ, the Josephson current ε, and dissipation ρ for the second resonance ($n=2$). Black curves refer to the absence of anisotropy parameters.

difference between SQUIDs with various phase shifts can be visible only in magnetic field. In order to calculate excess current dependence on magnetic field, we add squares of Eqs. (63) and (64). The resonant current is maximized when $\theta=\vartheta_+$ and we can write the solution in the parametric form

$$[I_{exc};\sin(\pi\phi_e + \vartheta_-)] = \left[\frac{\delta^2}{2\Gamma n};\frac{\delta}{\Gamma J_n^+(\delta)}\right], \tag{65}$$

where δ is a dummy variable. Changing the value of the parameter ϑ_- from 0 to $-\pi/2$, we have $0-0$ and $0-\pi$ SQUID, respectively. The shape of the surface describe current magnetic field dependence (see Fig. 10) remains unchanged but is translated by a vector $[0;-\vartheta_-]$ along the ϕ_e axis.

V. DISCUSSION

The resonances in SQUIDs are investigated theoretically with several asymmetries: Josephson current ϵ, dissipation ρ, and capacitance χ. In real devices, it is impossible to have an ideal interferometer free of imperfections. In practice, vari-

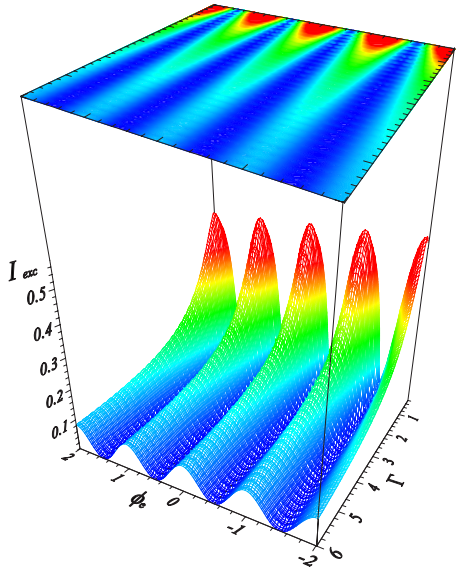

FIG. 10. (Color online) Excess current I_{exc} versus magnetic field ϕ_e (first resonance, $n=1$) characteristic for different values of the damping parameter Γ for the $0-\pi$ interferometer.

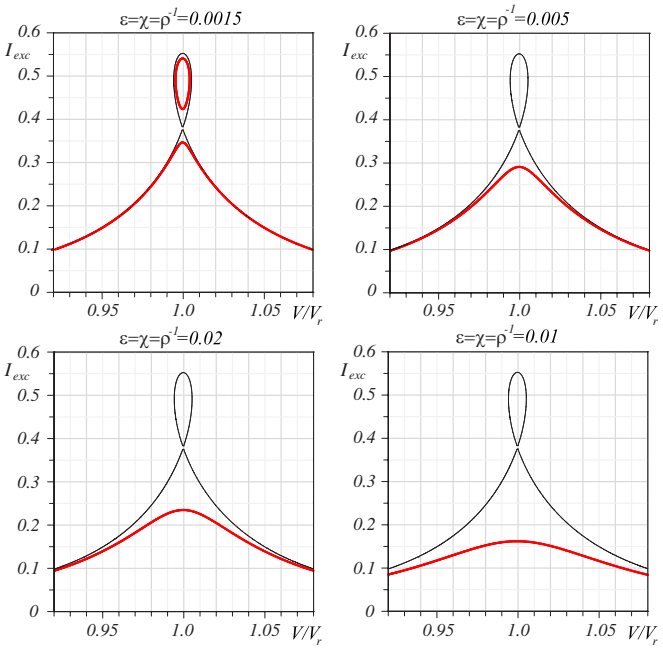

FIG. 11. (Color online) Current-voltage characteristics ($I_{exc}-V/V_r$) for several asymmetric configurations of the SQUIDs related to the Ambegaokar-Baratoff formula ($\Delta I_C \sim \Delta C \sim \Delta R^{-1}$) for changes of the junction area ΔA, for the first resonance $n=1$, $\Gamma=20$, and $\beta=0.1$.

ous deviations of the interferometer parameters from average values can occur together and mutually conceal each other. At this stage, we have to separate discussion related to low- and high-T_C SQUIDs. In the former case, experimentally, we are able to control asymmetry of dissipative parameter ρ by adding a parallel resistor to the junction but it is difficult to change the Josephson current independently of the capacitance. To produce the asymmetry of the Josephson current in the interferometer, we can change the area of the junction A or thickness of the barrier d. Parallel-plate capacitor with area A of the plates and space d between them has the capacitance equal to $C=\epsilon_r\epsilon_0 A/d$ for $A \gg d^2$, where ϵ_r is the relative dielectric constant of the interlayer dielectric and ϵ_0 is the vacuum electric constant. On the other hand, the critical current can be written as $I_C=j_C A$, where j_C is the critical current density. These two simple relations imply that varying area ΔA of the junction in the interferometer, we change both capacitance and critical current proportionally $\Delta I_C \sim \Delta C$ at the same time. When no further resistor is added to the junctions, not only capacitance and Josephson current are related. From the Ambegeokar-Baratoff[36] formula, we know that the product $I_C R_N$, where R_N is the resistance in normal state, has an invariant value which depends only on the material at fixed temperature. Thus, changing the value of the Josephson current, we alter the resistance of the junction. Recapitulating these rather simple considerations, we can introduce asymmetry in the Josephson current by changing the area of the junction ($\Delta I_C \sim \Delta C \sim \Delta R^{-1}$). Setting parallel resistor, we can control the value of the resistance and vary dissipative parameter independently of the current asymmetry. We can also imagine junctions with different thicknesses of the barrier but technologically this case is difficult to achieve, and thus we do not consider it. In experiments with ASQUID, both technically reached asymmetric cases do not differ very much because of the capacitance anisotropy. As we see in Fig. 11, the anisotropy of the capacitance has the biggest impact on the maximum value of the resonant current. Even small changes of χ can decrease excess current almost to zero.

The situation changes completely when high-T_C SQUIDs are considered. On one hand, the probability to find junction parameter asymmetries is particularly high, because high-T_C junctions are intrinsically affected by defects as, for instance, faceting and/or oxygen vacancies inside the barrier. Moreover, up to now, the charge transport process is not completely understood, although various hypotheses have been proposed,[37–39,41] and other recent experiments are still in progress.[18,40] In particular, the simple rule $I_C R_N$=const valid for low-T_C SQUIDs does not apply in the case of high-T_C interferometers typically used in applications, based on the symmetric bicrystal c-axis [001] devices, and changing one single parameter is now possible. In such interferometers, $I_C R_N$ is proportional to the critical current density J_C at low values and stays roughly constant at high-J_C values.[42,43] Moreover, HTS junctions are intrinsically shunted and SQUIDs are fabricated with no additional shunt resistor. As a consequence, the way to fabricate HTS SQUIDs with symmetric junctions is probably to reduce junctions' widths, limiting the effect of the interface defects. In all other cases, asymmetries will be very probable and our analysis could be relevant to understanding the presence of resonance steps.

Different approach is necessary in the case of asymmetric [001] or [100] HTS bicrystal junctions, where the relation $I_C R_N$ seems to be similar to the one of low-T_C systems[43] and the necessity to account for effects of a nonconventional symmetry of the order parameter forces one to also include the phase asymmetries in studying dynamical states in HTS interferometers. Finally, the inclusion of the second har-

monic term in the Josephson current in order to account for experimental results[44–46] is also mandatory. This will be the argument of a separate paper, and the possibility to deal with one single asymmetric parameter is now eventual. Moreover, a nonconventional symmetry of the order parameter forces one to also include phase asymmetries in studying dynamic states in high-T_C interferometers. In this frame, the calculations derived in the present paper allow the investigation of SQUID dynamics in both low- and high-T_C asymmetric devices.

VI. SUMMARY

In this paper, we have presented a detailed theoretical study of the resonances in the asymmetric superconducting quantum interference device. Analytical approach revealed the nature of the resonances in the presence of several asymmetries: Josephson current ϵ, capacitances χ, and dissipation ρ. Also, we were able to derive magnetic field dependence of the excess current in the presence of the magnetic field and phase shift. Our calculations imply that deviations of the capacitances from the average value in SQUID have profound impact on the physics of the system. We have found that our theory can be useful to determine asymmetry parameters present in lightly damped ASQUIDs. Specifically, for SQUIDs produced from HTS materials where deviations from average values are practically inevitable, our considerations are very helpful.

ACKNOWLEDGMENTS

The authors would like to thank Antonio Barone and Ciro Nappi for a lot of fruitful discussions. This work was supported by the TRN "DeQUACS."

[1] *Fundamentals, Fabrication and Applications*, edited by H. Weinstock, NATO Advanced Studies Institute, Series E: Applied Science Vol. 329 (Kluwer, Dordrecht, 1996).
[2] J. C. Mosher, E. R. Flynn, A. Quinn, A. Weir, U. Shahani, R. J. P. Bain, P. Maas, and G. B. Donaldson, Rev. Sci. Instrum. **68**, 1587 (1997).
[3] K. A. Kouznetsov, J. Borgmann, and John Clarke, Rev. Sci. Instrum. **71**, 2873 (2000).
[4] R. L. Fagaly, Rev. Sci. Instrum. **77**, 101101 (2006).
[5] N. Bergeala, J. Lesueur, G. Faini, M. Aprili, and J. P. Contour, Appl. Phys. Lett. **89**, 112515 (2006).
[6] T. Lindstrom, J. Johansson, T. Bauch, E. Stepantsov, F. Lombardi, and S. A. Charlebois, Phys. Rev. B **74**, 014503 (2006).
[7] C. H. Wu, M. J. Chen, J. C. Chen, K. L. Chen, H. C. Yang, M. S. Hsu, T. S. Lai, Y. S. Tsai, H. E. Horng, J. H. Chen, and J. T. Jeng, Rev. Sci. Instrum. **77**, 033901 (2006).
[8] H. C. Yanga, S. Y. Yang, G. L. Fang, W. H. Huang, C. H. Liu, S. H. Liao, H. E. Hornga, and Chin-Yih Hong, J. Appl. Phys. **99**, 124701 (2006).
[9] R. Gross, P. Chaudhari, M. Kawasaki, M. B. Ketchen, and A. Gupta, Appl. Phys. Lett. **57**, 727 (1990).
[10] M. Kawasaki, P. Chaudhari, T. H. Newman, and A. Gupta, Appl. Phys. Lett. **58**, 2555 (1991).
[11] K. Barthel, D. Koelle, B. Chesca, A. I. Braginski, A. Marx, R. Gross, and R. Kleiner, Appl. Phys. Lett. **74**, 2209 (1999).
[12] D. Koelle, Kleiner, F. Ludwig, E. Dantsker, and John Clarke, Rev. Mod. Phys. **71**, 631 (1999).
[13] Seung Kyun Lee, W. R. Myers, H. L. Grossman, H.-M. Cho, Y. R. Chemla, and John Clarke, Appl. Phys. Lett. **81**, 3094 (2002).
[14] Chiu-Hsien Wu, Hong-Chang Yang, Ji-Cheng Chen, Kuen-Lin Chen, M. J. Chen, J. T. Jeng, and Herng-Er Horng, J. Appl. Phys. **100**, 064510 (2006).
[15] M. Sigrist and T. M. Rice, Rev. Mod. Phys. **67**, 503 (1995).
[16] D. J. Van Harlingen, Rev. Mod. Phys. **67**, 515 (1995).
[17] C. C. Tsuei and J. R. Kirtley, Rev. Mod. Phys. **72**, 969 (2000).
[18] R. R. Schulz, B. Chesca, B. Goetz, C. W. Schneider, A. Schmehl, H. Bielefeldt, H. Hilgenkamp, J. Mannhart, and C. C. Tsuei, Appl. Phys. Lett. **76**, 912 (2000).
[19] Henk-Jan H. Smilde, A. Ariando, Horst Rogalla, and Hans Hilgenkamp, Appl. Phys. Lett. **85**, 4091 (2004).
[20] L. B. Ioffe, V. B. Geshkenbein, M. V. Feigel'man, A. L. Fauchere, and G. Blatter, Nature (London) **398**, 679 (1999).
[21] C. D. Tesche and J. Clarke, J. Low Temp. Phys. **29**, 301 (1977).
[22] G. Testa, C. Granata, C. Di Russo, S. Pagano, M. Russo, and E. Sarnelli, Appl. Phys. Lett. **79**, 3989 (2001).
[23] G. Testa, E. Sarnelli, S. Pagano, C. R. Calidonna, and M. Mango Furnari, J. Appl. Phys. **89**, 5145 (2001).
[24] A. Barone and G. Paterno, *Physics and Applications of the Josephson Effect* (Wiley, New York, 1982).
[25] H. H. Zappe and B. S. Landman, J. Appl. Phys. **49**, 344 (1978); **49**, 4149 (1978).
[26] D. B. Tuckerman and J. H. Magerlein, Appl. Phys. Lett. **37**, 241 (1980).
[27] S. M. Faris and E. A. Valsamakis, J. Appl. Phys. **52**, 915 (1981).
[28] C. Camerlingo, B. Ruggiero, M. Russo, and E. Sarnelli, J. Appl. Phys. **67**, 1987 (1990).
[29] B. Chesca, Ann. Phys. **8**, 511 (1999); Physica B **284**, 2124 (2000).
[30] B. Chesca and R. Kleiner, Physica C **350**, 180 (2001).
[31] B. Chesca, R. R. Schulz, B. Goetz, C. W. Schneider, H. Hilgenkamp, and J. Mannhart, Phys. Rev. Lett. **88**, 177003 (2002).
[32] K. K. Likharev, *Dynamics of Josephson Junction and Circuits* (Gordon and Breach, New York, 1984).
[33] M. Abramovitz and I. Stegun, *Handbook of Mathematical Functions* (Dover, New York, 1970).
[34] N. R. Werthamer and S. Shapiro, Phys. Rev. **164**, 523 (1967).
[35] P. Gueret, Appl. Phys. Lett. **35**, 889 (1979).
[36] V. Ambegaokar and A. Baratoff, Phys. Rev. Lett. **10**, 486 (1963).
[37] R. Gross and B. Mayer, Physica C **180**, 235 (1991); A. Marx, U. Fath, L. Alff, and R. Gross, Appl. Phys. Lett. **67**, 1929 (1995).
[38] E. Sarnelli, P. Chaudhari, and J. Lacey, Appl. Phys. Lett. **62**, 777 (1993); E. Sarnelli and G. Testa, Physica C **371**, 10 (2002).
[39] H. Hilgenkamp and J. Mannhart, Rev. Mod. Phys. **74**, 485 (2002), and references therein.
[40] C. W. Schneider, S. Hembacher, G. Hammerl, R. Held, A. Schmehl, A. Weber, T. Kopp, and J. Mannhart, Phys. Rev. Lett.

92, 257003 (2005).
[41] S. H. Mennema, J. H. T. Ransley, G. Burnell, J. L. MacManus-Driscoll, E. J. Tarte, and M. G. Blamire, Phys. Rev. B **71**, 094509 (2005).
[42] H. Hilgenkamp and J. Mannhart, Appl. Phys. Lett. **73**, 265 (1988).
[43] E. Sarnelli, G. Testa, D. Crimaldi, A. Monaco, and M. A. Navacerrada, Supercond. Sci. Technol. **18**, L35 (2005).
[44] E. Ilichev, V. Zakosarenko, R. P. J. Ijsselsteijn, H. E. Hoenig, V. Schultze, H. G. Meyer, M. Grajcar, and R. Hlubina, Phys. Rev. B **60**, 3096 (1999).
[45] T. Lindstrom, S. A. Charlebois, A. Ya. Tzalenchuk, Z. Ivanov, M. H. S. Amin, and A. M. Zagoskin, Phys. Rev. Lett. **90**, 117002 (2003).
[46] C. H. Gardiner, R. A. M. Lee, J. C. Gallop, A. Ya. Tzalenchuk, J. C. Macfarlane, and L. Hao, Supercond. Sci. Technol. **17**, 234 (2004).